nature photonics

ARTICLES

PUBLISHED ONLINE: 26 APRIL 2009 | DOI: 10.1038/NPHOTON.2009.68

Electrofluidic displays using Young–Laplace transposition of brilliant pigment dispersions

J. Heikenfeld[1]*, K. Zhou[1], E. Kreit[1], B. Raj[1], S. Yang[1], B. Sun[2], A. Milarcik[2], L. Clapp[2] and R. Schwartz[2]

Conventional electrowetting displays reconfigure the contact angle of a coloured oil film on a planar hydrophobic surface. We report on electrofluidic displays, in particular a three-dimensional microfluidic display device that provides a direct view of brilliantly coloured pigment dispersions. Electromechanical pressure is used to pull the aqueous dispersion from a reservoir of small viewable area (<10%) into a surface channel of large viewable area (>90%). The hydrophobic channel and reservoir respectively impart a small or large radius of curvature on the dispersion. Therefore, with no voltage, Young–Laplace pressure forces the dispersion to retract into the reservoir. Preliminary prototypes exhibit ∼55% white reflectance, and future development points towards a reflectance of ∼85%. Uniquely, compared to electrowetting pixels, the electrofluidic pixels reduce the visible area of the coloured fluid by an additional two to three times (improving contrast), are potentially bistable, are as thin as ∼15 μm (giving potential for rollable displays), and can be miniaturized without increased operating voltage.

Reflective displays use ambient light to illuminate the screen image and therefore provide superior energy efficiency, sunlight legibility, and flexible/rollable[1] form factor. Numerous technologies are vying for reflective applications: in electronic paper, high white state reflectance R (%) is critical, examples include electrophoretic[1] (E-Ink, ∼40%), electrowetting[2] (Liquavista, >50%), cholesteric liquid crystal[3] (Kent Displays Inc., ∼30%), electrochromic[4,5] (NTerra Inc., ∼45%, DIC, ∼65%), micro-electromechanical interference[6] (Qualcomm Inc., ∼25%) and liquid powder[7] (Bridgestone, ∼40%). However, all of these technologies fall well short of the visual brilliance and contrast of pigments printed onto bleached-wood fibre ($R > 80\%$). For example, electrophoretic displays and liquid powder displays are fundamentally limited by the need to place a thin white pigment layer in front of a black absorbing layer. Interference modulated displays can provide brilliant reflective colour at a single pixel, but creating a broadband and wide-angle white reflector is not achievable at the scales required for micro-electromechanical operation. Electrowetting displays currently achieve high reflectance by reconfiguring the contact angle of a coloured oil film on a planar white substrate. However, the coloured oil area is typically only reduced to ∼20–30% of the viewable area, limiting contrast. Furthermore, dyes generally lack the light stability and colour performance of pigments used in modern printed media. If reflective displays are to achieve the performance of paper, an altogether different approach will be required, and not just incremental improvements to existing technologies. Ideally, a new approach might leverage the use of high-performance pigments used in printing. Somehow, these pigments would need to be hidden to occupy less than 5–10% of the viewable area when paper-white reflection is desired. Furthermore, any new approach should use only planar photolithographic microfabrication so that the technique is suitable for manufacture.

Figure 1 presents a newly proposed 'electrofluidic' display structure that reduces the visible area of the coloured fluid by a factor of two to three more than that of an electrowetting display. The electrofluidic architecture is further distinct from electrowetting displays in its driving principles, device structure, its potential for bistability, the reduced parallax for multilayer subtractive colour pixels, its tight pixel confinement for rollable displays, and in its use of water-dispersed pigments instead of oil-soluble dyes. We chose 'electrofluidic' nomenclature because the mechanism involves charge-induced movement of liquids through microfluidic cavities.

The basic electrofluidic structure has several important geometrical features. The first is a reservoir that will hold an aqueous pigment dispersion in less than 5–10% of the visible area. The second feature is a surface channel occupying 80–95% of the visible area; this receives the pigment dispersion from the reservoir when a suitable stimulus is applied. Third, there is a duct surrounding the device that enables counterflow of a nonpolar fluid (oil or gas) as the pigment dispersion leaves the reservoir. It is important to note that all of these features are inexpensively formed in a single photolithographic or microreplication step. Several additional coatings and a top substrate are added (Fig. 1b). The surface channel is first bound by two electrowetting[8] plates consisting of an electrode and hydrophobic dielectric. The top electrowetting plate is composed of a transparent In_2O_3:SnO_2 electrode (ITO) so that the surface channel may be viewed by the naked eye. The bottom electrowetting plate comprises a highly reflective electrode made from aluminium, for example. With this arrangement, when no voltage is applied, a net Young–Laplace pressure[9] causes the pigment dispersion to occupy the cavity, which imparts a larger radius of curvature on the pigment dispersion. Therefore at equilibrium, the pigment dispersion occupies the reservoir and is largely hidden from view. This is analogous to connecting two soap bubbles by a straw—the larger bubble has a larger radius of curvature and a lower Young–Laplace pressure, and will therefore consume the smaller bubble. When a voltage is applied between the two electrowetting plates[10] and the pigment dispersion (Fig. 1c), an electromechanical[11] pressure is induced that exceeds the net Young–Laplace pressure, and the pigment dispersion is pulled into the surface channel. If the volume of the pigment dispersion is slightly greater than the volume of the surface channel, then the pigment will be simultaneously viewable in both the reservoir and the surface channel, and nearly the entire device area will exhibit the coloration of the pigment. If the voltage is removed the pigment dispersion rapidly (milliseconds to tens of milliseconds) recoils into the reservoir. Thus a switchable

[1]Novel Devices Laboratory, Department of Electrical and Computer Engineering, University of Cincinnati, Cincinnati, Ohio 45221, USA, [2]Sun Chemical Corporation, Cincinnati, Ohio 45232, USA. *e-mail: heikenjc@email.uc.edu

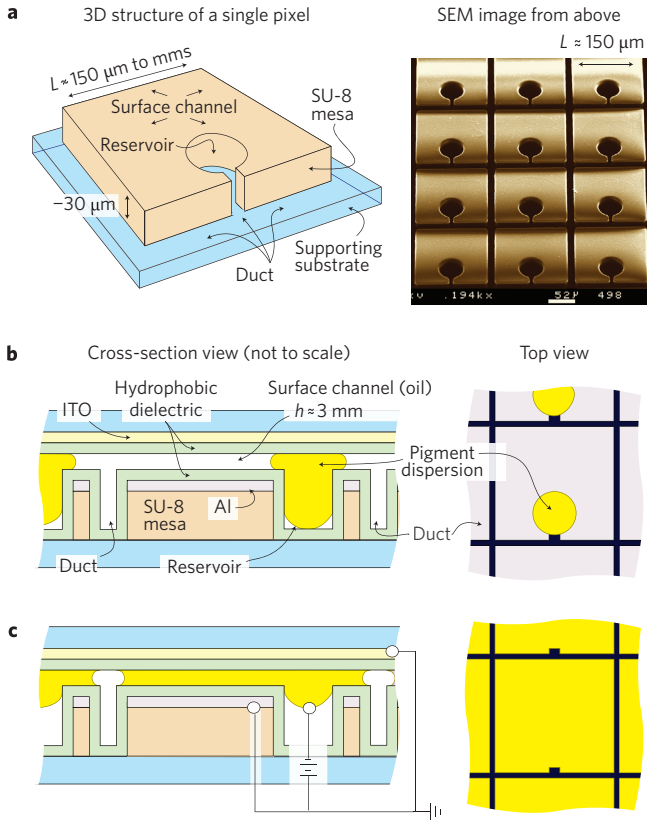

Figure 1 | The three-dimensional pixel structure and basic pixel operation. **a**, Three-dimensional diagram of a single pixel (left) and scanning electron microscope (SEM) images (right) of the SU-8 mesa structure. **b**,**c**, Cross-sections (left) and top views (right) of the pixels with no voltage (**b**) and an applied voltage (**c**) sufficient to cause the pigment dispersion to fill the surface channel.

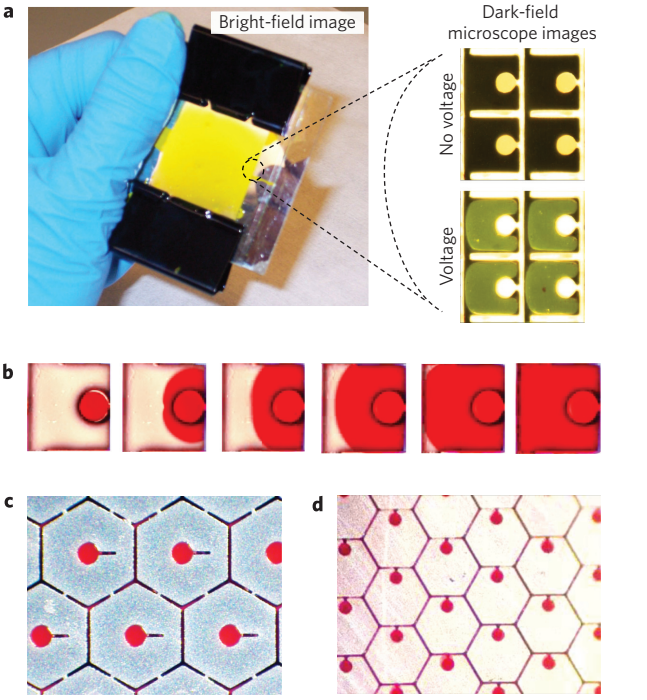

Figure 2 | Images of electrofluidic displays and pixels. **a**, Bright-field image of a 170 DPI direct-drive demonstrator with ~30,000 pixels (left) and pixel dark-field images (right). **b**, Time-lapse images of 500-μm-square pixels. **c**, Hexagonal pixel with two separate ducts, one for the reservoir and one for the pixel border. **d**, Hexagonal pixels in which the reservoir comprises only ~5% of the viewable area. Two videos of pixel operation are also provided in the Supplementary Information.

device is created that can hide the pigment or reveal the pigment with a visual brilliance that is similar to pigment printed on paper. Figure 2a presents a bright-field photograph of an assembled yellow prototype and dark-field microscope images of individual pixels. Dark-field imaging only captures scattered light from nonplanar or diffuse surfaces, and therefore highlights the self-diffuse (optically scattering) advantage of pigment dispersions. Shown in Fig. 2b–d are bright-field images of several red pigment and alternative device geometries. (See Supplementary Information for two dark-field videos of $L \approx 150$ and 300 μm pixels.) Single pixels can be as small as tens of micrometres, and in our laboratory we have demonstrated reversible switching over surface channel lengths as large as 100 cm. It is interesting to briefly note that pigment area is changed in a manner that visually mimics biological chromatophores[12] in bobtail squids[13] and chameleons.

A deeper discussion of the fundamental operating principles will now be presented. Figure 3a schematically demonstrates that the movement of pigment dispersion into or out of the surface channel is regulated by a competition between Young–Laplace pressure[9] and electromechanical[11] pressure generated by the electrowetting effect[8]. Young–Laplace pressure can be calculated from

$$\Delta p = \gamma_{ao}(1/R_1 + 1/R_2) \quad (1)$$

which includes interfacial surface tension γ_{ao} between the aqueous pigment dispersion and the oil, and the principle radii of curvature for the pigment dispersion meniscus (R_1, R_2). Typical pixels have a surface channel length ($L \approx 50$–500 μm) that is $\gg 10\times$ the channel height h. Therefore, Young–Laplace pressure in the surface channel is dominated by only a single radius of curvature R. For the materials used herein, the Young's contact angle[9] θ_Y for the pigment dispersion is $>160^\circ$, and therefore R can be further approximated as being only due to the surface channel height ($R \approx h/2$). The pigment dispersion also has a curved meniscus in the reservoir, where the radius of curvature is governed by two equal radii of curvature. However, the reservoir diameter is typically $>10\times$ the surface channel height and the Young–Laplace pressure in the reservoir is insignificantly small. Therefore at no voltage the net Young–Laplace pressure can be approximated as being due only to the surface channel: $\Delta p \approx 2\gamma_{ao}/h$. As shown in the plot of Fig. 3a, at no voltage an example device has a maximum Δp of ~3 kN m^{-2}. For the case for applied voltage an understanding of the electrowetting[8] effect is first required:

$$\cos\theta_V = \cos\theta_Y + \frac{1}{2}\frac{\varepsilon V^2}{\gamma_{ao} d} \quad (2)$$

where θ_V is the electrowetted contact angle, ε/d is the hydrophobic dielectric capacitance per unit area, and the applied d.c. voltage or a.c. r.m.s. voltage is indicated by V. As predicted by equation (2) and as shown in Fig. 3a, electrowetting reduces the pigment dispersion contact angle as the voltage is increased. Combining equations (1) and (2), the net pressure acting on the pigment dispersion in the surface channel can be approximated as

$$\Delta p \approx \frac{2\gamma_{ao}}{h} - \frac{\varepsilon V^2}{hd} \quad (3)$$

As shown in the plot and diagrams of Fig. 3a and according to equation (3), the pigment dispersion will be pulled into the

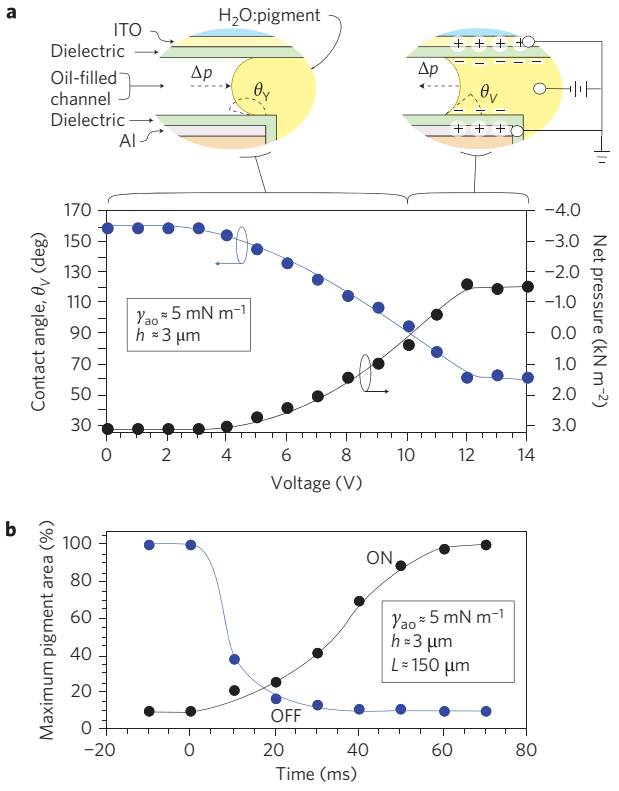

Figure 3 | Voltage and time response of electrofluidic pixel characteristics. **a**, Plot of contact angle and net meniscus pressure versus voltage, and schematic of the pigment dispersion movement in the surface channel. **b**, Pigment area versus time for 150-μm pixels.

surface channel when Δp becomes negative. Without substantial contact angle hysteresis[9], equation (2) also predicts that the threshold for pulling pigment into the surface channel is $\theta_V < 90^\circ$ (analogous to capillary wetting). For the materials used in Fig. 3, the pressure pulling the pigment dispersion into the surface channel reaches a maximum at the onset of electrowetting saturation ($V \approx 12$ V, $\theta_V \approx 60^\circ$, $h \approx 3.0$ μm, $\gamma_{ao} \approx 5$ mN m^{-1}, $\Delta p \approx -1.5$ kN m^{-2}). The electrowetting saturation is likely due to charge injection[14] into the hydrophobic dielectric. Preliminary tests were also performed with alternative aqueous/oil/dielectric materials and with ~30–100 Hz bipolar voltages like those used in displays. These tests showed less charge injection and contact angles as low as $\theta_V \approx 30^\circ$ (with a larger range for Δp). Higher surface tension can also be used to achieve values of Δp of ~–17 kN m^{-2}, as demonstrated with d.c. voltage and a carbon black pigment dispersion ($\theta_V \approx 70^\circ$, $h \approx 2.0$ μm, $\gamma_{ao} \approx 50$ mN m^{-1}). We have also recently validated full pixel ON/OFF contrast for a materials system with a value of $\theta_Y \approx 105^\circ$ and $\theta_V \approx 75^\circ$. We note this achievement because electrofluidic pixels therefore require less contact angle change than conventional electrowetting pixels ($\theta_Y \approx 180^\circ$, $\theta_V \approx 90$–120°). Furthermore, unlike electrowetting pixels, electrofluidic pixels do not require increased operating voltage as the pixel size is scaled down[15]. These opportunities for reduced operating voltage (electric field) are important because they can reduce the occurrence of electrolysis (dielectric breakdown).

For all the examples discussed above, the duct design shown in Fig. 1a has been effective at terminating advancement of the pigment dispersion at the end of the surface channel. The physics governing this termination has two origins: (i) the duct marks the end of the aluminium electrode; (ii) the dispersion encounters a diverging capillary geometry at the channel/duct interface. Thus the duct is further important as it prevents merging of pigment dispersions in adjacent pixels. Regarding intermediate pigment positioning (grey scale), for voltages implemented near the ideal threshold of $\Delta p = 0$ the pigment dispersion could be held at various positions. The voltage range for stability can be determined from equation (3) by incorporating the effects of contact angle hysteresis[8,9]. Contact angle hysteresis is typically only a few degrees in oil (<0.1–1 kN m^{-2}), but it can be increased by providing a rough or patterned hydrophobic dielectric (~1s of kN m^{-2}).

We will now provide a proper explanation of why the pushing and pulling of the pigment dispersion should be considered as the result of the net pressure between Young–Laplace and electromechanical pressure. It has been experimentally demonstrated[16] that the local microscopic contact angle at the contact line is always Young's (θ_Y). The electrowetted contact angle (θ_V) is only a projection that is macroscopically observed at a distance from the solid surface that is roughly equal to the hydrophobic dielectric thickness (d). Therefore, for the surface channel geometries used herein ($h \approx$ 1s of micrometres) and dielectric thicknesses ($d \approx$ 0.1s to 1s of micrometres), the meniscus geometry will exhibit a more complex curvature than the simple diagram shown in Fig. 3a. Consequently, it is appropriate to use equations (2) and (3), but with the understanding that movement of the pigment dispersion with voltage should not be directly attributed to contact angle change. Some further clarifications are provided. At 12 V the total electromechanical pressure is approximately –4.5 kN m^{-2}, which simply exceeds the ~3.0 kN m^{-2} Young–Laplace pressure, resulting in a net pressure of approximately –1.5 kN m^{-2}, as shown in Fig. 3. We previously stated that our maximum achievable net pressure was approximately –17 kN m^{-2}. This net pressure is the sum of ~50 kN m^{-2} Young–Laplace pressure and approximately –67 kN m^{-2} electromechanical pressure. These descriptions are all consistent with equation (3).

This understanding of pressure is critical to the next topic of discussion: the potential for video switching speed (~10–20 ms). As shown in Fig. 3b, the demonstrated ON speed for filling 90% of the maximum pigment area is currently $t_{ON} \approx 50$ ms for 150-μm electrofluidic display pixels. It is notable that the OFF speed in Fig. 3b is ~2× faster than the ON speed, which is in agreement with the ~2× difference in magnitude of Δp shown in Fig. 3a. Next, consider theoretical speed for 170 DPI colour pixels, where the RGB subpixel size would be $L \approx 50$ μm. As a first approximation, this smaller L will decrease t_{ON} by ~9× as the distance travelled is reduced by 3× and as the liquid velocity U is increased 3× according to $U \propto h/L$ (ref. 17). t_{ON} could also be decreased by ~10× through previously mentioned materials that yield $\Delta p \approx 17$ kN m^{-2}. Now, consider how the current $t_{OFF} \approx 25$ ms would be affected by scaling and materials optimization. Again, device scaling to $L \approx 50$ μm provides a 9× decrease in t_{OFF}, and the case for an optimized Δp provides a ~15× decrease in t_{OFF} ($\Delta p \approx$ –50 kN m^{-2}). Finally, the oil and pigment viscosities are ~2 cSt and could be potentially reduced to ~1 cSt, resulting in a 2× decrease in both t_{ON} and t_{OFF}. The net effect of the above design changes predicts a minimum t_{ON} and t_{OFF} that is well below 1 ms. Such speed is far faster than that required for video, and only a small fraction of the abovementioned improvements are needed.

Our last detailed discussion is on display brightness as determined by pigments, reflectors, fill factor and pixel architecture. Brilliant coloration is achieved by transposing a ~10–15 wt% pigment dispersion in front of a high-performance reflector such as aluminium. This approach is conceptually unique and has several advantages over other pigment-based display devices such as electrophoretic[1] or liquid powder[7] displays. It should be noted that electrofluidic devices can also operate with the dye-coloured oil and clear water used in electrowetting displays[2]. However, aqueous pigment dispersions provide a significant performance boost over dyes[2] for the following reasons: (i) they are self-diffuse

(optically scattering) for an inherently wide view angle; (ii) they generally provide superior light fastness due to reduced surface area exposure to oxygen, light or water[18]; (iii) at high concentrations (>10 wt%) pigment dispersions typically allow a wider range of interfacial surface tension (γ_{ao} ~5 to ~50 mN/m) than dyes in oil[19]; (iv) pigments are aqueous-dispersed, so even at ~10 wt% a very low viscosity is achieved (~2 cSt); (v) unlike coloured oil, coloured water allows electrically conductive colorants such as carbon-black to be used. The custom pigment dispersions developed for electrofluidic displays were provided by Sun Chemical Corp. A diffusely reflective white state is also required for a wide viewing angle. Although not shown here, diffuse white coloration can be achieved by using a diffuse or translucent oil, by using a textured aluminium reflector, or by using the ~tens of micrometres thickness of the polymer mesa to build up a diffusely reflecting layer. For a maximally bright white or coloured state, a high-performance reflector is required. An aluminium reflector system is used for the device shown in Fig. 2. When dielectric-protected, this aluminium reflector has a measured R of >93%. Even higher reflectivity is possible if the aluminium is placed beneath a mesa or dielectric containing $BaTiO_3$ powder. Also, $R > 98\%$ across the visible spectrum is available with a multilayer polymer dielectric reflector similar to 3M Vikuiti ESR. Consider a 150-μm-wide pixel (L), with a surface channel height of 3 μm (h), and with a 2-μm-wide duct (regarding fabrication challenges, the duct does not need to reach all the way to the lower substrate). An aluminium reflector can enable a white state reflectance of $R > 77\%$ or >90% as theoretically calculated for a ratio of surface channel to reservoir area of 10:1 or 20:1, respectively. For a carbon-black pigment dispersion with <5% reflectance, the theoretical contrast ratio can therefore range from >15:1 to >18:1. Interestingly, conventional offset printed ink films are ~2 μm thick and may typically contain about 15–25% pigment. Therefore the combination of pigment loading and thickness of the electrofluidic pixel can provide a degree of saturation similar to conventional printed media. It should be noted that to achieve such performance the films on the top substrate must be optimized in thickness and refractive index to minimize Fresnel reflections. Although we have not yet optimized the reflective aluminium electrode, the top substrate, or pixel geometry for ~80–90% white reflectance, we can report on preliminary prototype results. 1-inch diagonal direct-drive prototypes have been demonstrated at pixel sizes of a few millimetres, 500 μm, 300 μm and 150 μm (~30,000 pixels). Greater than 98% pixel yield has been achieved at the 300 μm pixel size. Several combinations of white diffuse, coloured (C, M, Y or R), and opaque black (K) liquids have been tested. Prototypes with ~300-μm pixels already provide a switchable white/black reflectivity of ~55%/~8% (~7:1). The development tasks for achieving >80% reflectivity and ~20:1 contrast ratio are a fairly straightforward improvement of existing device features: the aluminium reflector ($R \approx 70\%$), the reflective area (~75%), and the antireflection coating of the front glass ($R \approx 5\%$). Progress is under way, as recent single pixel tests now show >90% reflective area. Full-colour operation requires a more sophisticated pixel architecture. As illustrated in Fig. 4a, a high-efficiency black/white electrofluidic pixel can be combined with a RGBW colour filter array[20]. This could theoretically result in a ~40% white state brightness (like the existing Amazon Kindle™ but with the advantage of offering full colour images). Also shown in Fig. 4a, an even higher full-colour brightness of >60% is theoretically possible if a two-layer subtractive CMY approach is used, similar to that that proposed for electrowetting[2] cholesteric[21] displays. The electrofluidic CMY pigment dispersions developed by Sun Chemical have the spectra shown in Fig. 4b, and are shown in Fig. 4c. It should be noted for the two-layer CMY approach that the geometry and coloured fluid positioning in electrofluidic pixels is further distinct from electrowetting pixels

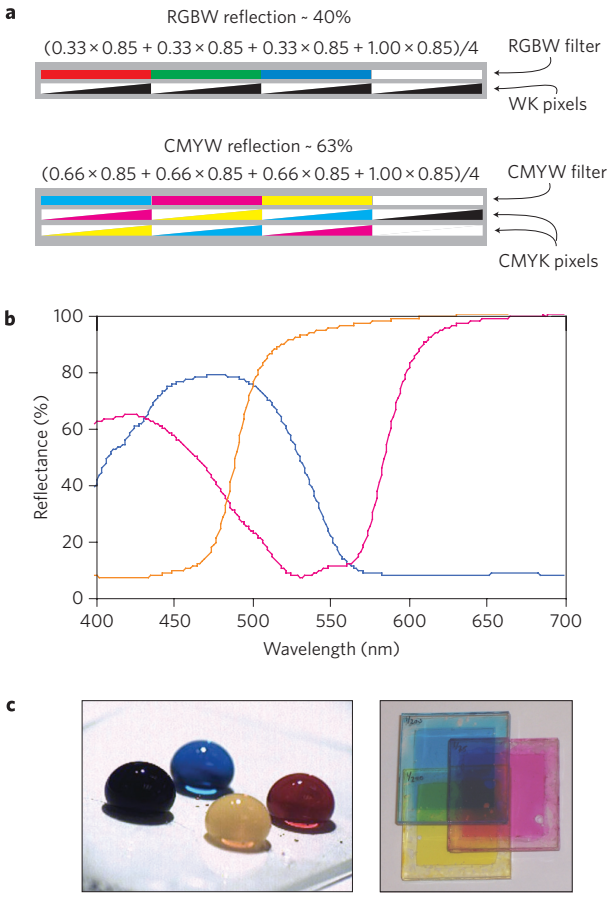

Figure 4 | Colour filtering techniques and materials that are required for full-colour electrofluidic displays. a, Red-green-blue-white[20] (RGBW) and cyan-magenta-yellow-white (CMYW) pixel architectures. **b**, CMY pigment reflectance spectra. **c**, Images of pigment droplets and an overlay of three CMY prototypes.

in terms of parallax. For 300 DPI electrofluidic pixels the theoretical view angle is >45° before ~10% parallax arises. Although substantially more difficult to manufacture, use of three stacked CMY electrofluidic pixels is possible. The brightness of such an approach could equal that of printed media, but is likely limited to larger sized pixels such as those used in signage and indicators.

Thus far we have discussed the positive benefits and potentials for electrofluidic displays. However, research and development challenges should be briefly presented. First, the simple drive scheme shown in Fig. 1 does not provide analogue grey scale. Challenges to grey-scale operation include error accumulation (as in electrophoretic displays) and pixel capacitance that varies with grey-scale state (as in electrowetting displays). Therefore patterned electrodes or surfaces should be implemented for an analogue response or to create intermediate grey-scale reset states. Several simple yet promising grey-scale architectures are now in development. For electronic paper, bistable grey scale is highly desirable to eliminate power consumption once an image is selected. 'Droplet-driven' electrowetting displays[22] are bistable, but only allow two-bit grey scale. Advanced electrofluidic pixel concepts can theoretically provide bistable operation and analogue (numerous) grey-scale states. Regarding aging, electrolysis (dielectric breakdown) must be avoided, and as previously discussed there may be a lower voltage (electric field) advantage over conventional electrowetting displays. For applications such as rollable displays, adherent substrate spacers[23] comprising ~1–3% of the pixel area must be developed. Creating a full-colour reflective display is a highly challenging task for any technology, let alone

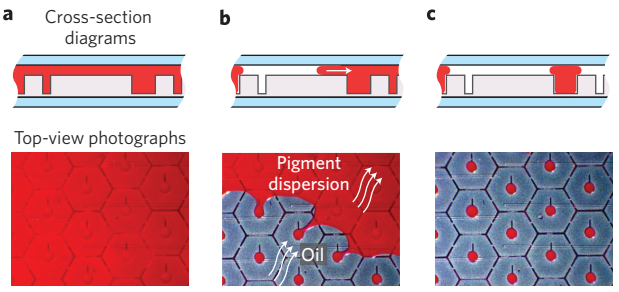

Figure 5 | The liquids in electrofluidic displays can be dosed by means of self-assembly. a,**b**, The pigment dispersion is first vacuum filled (**a**) similar to liquid dosing in a liquid-crystal display, then oil is introduced (**b**) at one edge of the display and the pigment recedes from the channel due to Young–Laplace pressure. However, the oil in the channel moves past the reservoir before pigment is removed from the reservoir (the reservoir has a larger cavity and lower Young–Laplace pressure). **c**, The completed dosing. A video of the liquid dosing is provided in the Supplementary Information.

electrofluidic displays, which have numerous geometries and materials not previously seen in displays. Full-colour operation requires repeatable liquid dosing. As shown in Fig. 5 we have developed a simple liquid self-assembly process that is governed by Young–Laplace pressure. The self-assembly process works well for the 1-inch demonstrator units, and scalability to larger sizes is in development. (See Supplementary Information for a video of the self-assembly process.) In addition to liquid dosing, we have made substantial efforts to ensure manufacturability. As detailed in the Methods, pixel fabrication only requires simple vacuum deposition, photolithography and wet-processing techniques. It is also interesting to note that the fabrication of the bottom substrate is identical in composition and number of steps to the fabrication of low-cost electrowetting displays[15], with only the geometry and sequencing of materials being different. Taking these challenges into account, we are now beginning to develop a more advanced prototype to fully demonstrate that electrofluidic displays can achieve performance equivalent to the centuries-old brilliance of pigments printed on paper.

Methods

The simplest embodiment of a direct-drive electrofluidic prototype was fabricated as follows. The entire process can be implemented with temperatures as low as ~100–120 °C and is likely compatible with organic transistors and flexible plastic substrates. First, Microchem SU-8 epoxy was photolithographically patterned to create the mesa structure shown in Fig. 1. As an alternative, the mesa structure can be created more quickly and at lower cost by using embossing/microreplication techniques similar to Sipix Microcup™ technology. Next, a reflective aluminium electrode and a dielectric such as Al_2O_3 or Parlyene C was vacuum deposited. The electrode was patterned and pixilation created by using angled deposition or photoresist patterning and wet-etching. These films were then further solution coated with Cytonix Fluoropel 1601V or Asahi Cytop 809M fluoropolymer. The dielectric and fluoropolymer comprise the hydrophobic dielectric shown in Figs 1 and 3. The array of pixels was dosed with dodecane oil and a ~10–15 wt% pigment dispersion provided by Sun-Chemical Corp. The liquid dosing, as shown in Fig. 5, uses a new self-assembly approach that expands upon our existing self-assembly capabilities[15] for electrowetting displays. The top substrate, which seals the device, included a ~50-nm thin In_2O_3:SnO_2 film and another hydrophobic dielectric. The top plate further included a patterned SU-8 spacer to regulate the surface channel height. Devices were temporarily sealed with rubber gaskets and binder-clips or permanently sealed with UV epoxy.

Received 6 October 2008; accepted 23 March 2009; published online 26 April 2009

References

1. Huitema, H. E. A. *et al.* Flexible electronic-paper active-matrix displays. *J. Soc. Inf. Display* **14,** 729–733 (2006).
2. Hayes, R. A. & Feenstra, B. J. Video-speed electronic paper based on electrowetting. *Nature* **425,** 383–385 (2003).
3. Khan, A. *et al.* Reflective cholesteric LCDs for electronic paper applications. *Proc. International Display Manufacturing Conference* 397–399 (2005).
4. Back, U. *et al.* Nanomaterials-based electrochromics for paper-quality display. *Adv. Mater.* **14,** 845–848 (2002).
5. Nakashima, M. *et al.* Naturally white electrochromic display using organic/inorganic nanocomposite pulp. *SID Symp. Dig.* **36,** 1678–1681(2005).
6. Miles, M. *et al.* Digital paper for reflective displays. *J. Soc. Inf. Display* **11,** 209–215 (2003).
7. Hattori, R. *et al.* A novel bistable reflective display using quick-response liquid powder. *J. Soc. Inf. Display* **12,** 75–80 (2004).
8. Mugele, F. & Baret, J. Electrowetting: from basics to applications. *J. Phys. Condens. Matter* **17,** R705–R774 (2005).
9. Berthier, J. *Microdrops and Digital Microfluidics* (William and Andrew, 2008).
10. Fair, R. Digital microfluidics: is a true lab-on-a-chip possible? *Microfluidics Nanofluidics* **3,** 245–281 (2007).
11. Jones, T. B. An electromechanical interpretation of electrowetting. *J. Micromech. Microeng.* **15,** 1184–1187 (2005).
12. Hanlon, R. T. & Messenger, J. B. *Cephalopod Behaviour* (Cambridge Univ. Press, 1998).
13. Kramer, R. M., Crookes-Goodson, W. J. & Naik, R. R. The self-organizing properties of squid reflectin protein. *Nature Mater.* **6,** 533–538 (2007).
14. Verheijen, H. & Prins, M. Reversible electrowetting and trapping of charge: model and experiments. *Langmuir* **15,** 6616–6620 (1999).
15. Sun, B. *et al.* Scalable fabrication of electrowetting displays with self-assembled oil dosing. *Appl. Phys. Lett.* **91,** 011106 (2007).
16. Mugele, F. & Buehrle, J. Equilibrium drop surface profiles in electric fields. *J. Phys. Condens. Matter* **19,** 375112 (2007).
17. Song, J., Evans, R., Lin, Y. Y., Hsu, B. N. & Fair, R. A scaling model for electrowetting-on-dielectric microfluidic actuators. *Microfluidics Nanofluidics* http://dx.doi.org/10.1007/s10404-008-0360-y (2009).
18. Cristea, D. & Vilarem, G. Improving light fastness of natural dyes on cotton yarn. *Dyes and Pigments* **70,** 238–245 (2006).
19. Roques-Carmes, T. *et al.* The effect of the oil/water interfacial tension on electrowetting driven fluid motion. *Colloids Surf. A* **267,** 56–63 (2005).
20. Brown Elliot, C., Credelle, T. & Higgins, M. Adding a white subpixel. *Inf. Display* **5,** 26–31 (2005).
21. Shiyanovskaya, I. *et al.* Single substrate coatable multicolor cholesteric liquid crystal displays. *Proc. Soc. Inf. Display* **38,** 65–68 (2007).
22. Blankenbach, K. *et al.* Novel highly reflective and bistable electrowetting displays. *J. Soc. Inf. Display* **16,** 237–244 (2008).
23. Jang, S. *et al.* Tight bonding of two plastic substrates for flexible LCDs. *Proc. Soc. Inf. Display* **38,** 653–656 (2007).

Acknowledgements

The authors acknowledge partial financial support for Cincinnati's general program in displays by Sun Chemical Corp., Motorola (K. Dean), Polymer Vision (E. Huitema), ITRI Taiwan (W. Cheng), Air Force Research Labs (R. Naik), Air Force Office of Scientific Research (AFOSR) Young Investigator Award no. 06NE223 (K. Reinhardt), and an National Science Foundation (NSF) CAREER Award no. 0640964 (Electronics Photonics & Device Technologies (EPDT)). The authors thank R. Fair of Duke University for discussion on switching speed in microscale electrowetting cavities.

Additional information

Supplementary information accompanies this paper at www.nature.com/naturephotonics. The authors declare competing financial interests: details accompany the full-text HTML version of the paper at www.nature.com/naturephotonics. Reprints and permission information is available online at http://npg.nature.com/reprintsandpermissions/. Correspondence and requests for materials should be addressed to J.H.